

Available online at [www.sciencedirect.com](http://www.sciencedirect.com)

ScienceDirect

<http://www.elsevier.com/locate/biombioe>

# Estimating biomass on CRP pastureland: A comparison of remote sensing techniques

Tucker F. Porter<sup>a</sup>, Chengci Chen<sup>b,\*</sup>, John A. Long<sup>c</sup>, Rick L. Lawrence<sup>c</sup>,  
Bok F. Sowell<sup>a</sup>

<sup>a</sup> Department of Animal and Range Sciences, Montana State University, P.O. Box 172900, Bozeman, MT 59717, USA

<sup>b</sup> Montana State University, Central Agricultural Research Center, 52583 US Highway 87, Moccasin, MT 59462, USA

<sup>c</sup> Department of Land Resources and Environmental Sciences, Montana State University, P.O. Box 173120, Bozeman, MT 59717, USA

## ARTICLE INFO

### Article history:

Received 29 October 2013

Received in revised form

27 January 2014

Accepted 31 January 2014

Available online 21 February 2014

### Keywords:

Biomass estimation model

NDVI

Bandwise regression

Crop circle sensor

Landsat imagery

## ABSTRACT

Biomass from land enrolled in the Conservation Reserve Program (CRP) is being considered as a biofuel feedstock source. A quick, accurate and nondestructive method to estimate biomass yield would be valuable for land managers to ensure sustainable production. The purpose of this study was to compare the ability of regression models to estimate biomass yields using data from satellite and ground based remote sensing platforms. Biomass yields and plant spectral responses were obtained at different phenological stages over two growing seasons (2011–2012) on an 8.1 ha CRP pasture in central Montana. Regression models were constructed using the normalized difference vegetation index (NDVI) and various band combinations from a hand held Crop Circle sensor and from Landsat satellite images. All models showed reasonable accuracy in estimating biomass, with a difference of <276 kg ha<sup>-1</sup> or 8% of measured values. None of the models showed statistically significant differences ( $p > 0.05$ ) between actual and estimated biomass. Results suggest that the usefulness of the spectral regions is a function of phenological growth stage. Red, red edge, and the near-infrared bands are more responsive at boot and peak growth stages while bands in the short-wave infrared increased the accuracy for the dormant stage biomass estimations. Land managers may construct spectral models to more effectively manage biomass resources.

© 2014 Elsevier Ltd. All rights reserved.

## 1. Introduction

The Biomass Research and Development Technical Advisory Committee established national goals in 2003 that biomass would supply 5% of the nation's total power, 20% of transportation fuels, and 25% of chemicals by 2030 [1]. Biomass

derived from land enrolled in the CRP, a voluntary program in which environmentally sensitive agricultural land is converted to vegetative cover, is being evaluated as a potential biofuel feedstock source to meet these goals [1–3]. CRP land in the United States totaled approximately 126,000 km<sup>2</sup> in 2010 [3], from which an estimated 15.4–25.4 Tg of dry biomass could be available for bioenergy production [2,4].

Abbreviations: CRP, conservation reservation program; NDVI, normalized difference vegetation index.

\* Corresponding author.

E-mail addresses: [tucker.f.porter@gmail.com](mailto:tucker.f.porter@gmail.com) (T.F. Porter), [cchen@montana.edu](mailto:cchen@montana.edu) (C. Chen), [john.long5@msu.montana.edu](mailto:john.long5@msu.montana.edu) (J.A. Long), [rickl@exchange.montana.edu](mailto:rickl@exchange.montana.edu) (R.L. Lawrence), [bok@montana.edu](mailto:bok@montana.edu) (B.F. Sowell).

0961-9534/\$ – see front matter © 2014 Elsevier Ltd. All rights reserved.

<http://dx.doi.org/10.1016/j.biombioe.2014.01.036>

CRP land is often environmentally fragile with a high degree of spatial variation in vegetative cover and soil types. It is critical, therefore, to develop methods that can accurately and nondestructively measure biomass in order to ensure sustainable production, harvesting, and soil protection. Remote sensing of vegetation from ground or satellite-based sensors might provide a tool to estimate biomass at management relevant scales [5]. The spectral response of plants has been found to change as they progress through different phenological growth stages [6,7]. Vegetation at different phenological stages differs in chemical composition and in morphology [8]. As plants mature, for example, the stem to leaf ratio and the amounts of lignin, cellulose, and hemicellulose all increase. These increases are accompanied by a simultaneous decrease in the amount of chlorophyll [8–10]. Plant phenology or growth stage is affected by environmental factors, such as photoperiod, temperature, and precipitation [11].

The Normalized Difference Vegetation Index (NDVI), developed to take advantage of specific reflectance properties of active photosynthetic plant tissue in the red and near-infrared portions of the electromagnetic spectrum, is a common remote sensing index used in agricultural studies [12]. Studies have shown that NDVI is well-correlated with total biomass [13], yields for specific crops, such as corn (*Zea mays* L.) and winter wheat (*Triticum aestivum* L.) [14,15], as well as biomass in vineyards [16], perennial grassland [17], pastureland [18], and shortgrass steppes [7]. Despite these studies, the strength of the relationship between NDVI and biomass might be reduced by the presence of dead or dormant plant material [7,19,20], which is often present in CRP land.

Another common remote sensing technique is bandwise regression – a specific case of stepwise multiple regression in which the explanatory variables are measures of reflected energy in sensor-specific spectral bands. It begins with a regression model built using all available spectral bands, and then the least significant bands are removed one at a time until the fit of the model no longer improves (e.g. [13,21]). Modeling biomass with bandwise regression was found to explain more variability than models based solely on NDVI in a highly disturbed landscape ( $R^2 = 0.75$  versus 0.65) [21] and in rangelands ( $R^2 = 0.66$  versus 0.41) [13]. Consequently, bandwise regression modeling is considered to be a more reliable technique to estimate biomass across landscapes with a high degree of variability in vegetative cover and soil types [13,21].

The purpose of this study was to compare the ability of bandwise and NDVI-based regression models to estimate biomass yields using data from satellite- and ground-based remote sensing platforms. The goal is to develop a method to quickly, accurately, and nondestructively estimate biomass in CRP pastureland at different phenological stages across multiple growing seasons in central Montana.

## 2. Methods

### 2.1. Study area

The study was conducted during the 2011 and 2012 growing seasons on 8.1 ha of CRP pastureland in Benchland, Montana, near the Montana State University Central Agricultural

Research Station (CARC) (Judith Basin County, 47°05'21" N, 110°00'44" W). The precipitation amounts during the 2011 and 2012 growing seasons (Fig. 1) were markedly different. In 2011 the study area received 8 cm more precipitation than the long-term (based on 103 yrs) annual average of 40 cm, while 2012 was substantially drier, receiving only 28 cm of precipitation [22]. The soil is a fine clay-loam (fine-loamy, carbonatic, frigid Typic Calciborolls) [23] and the dominant plant species are intermediate wheatgrass (*Thinopyrum intermedium* (Host) Barkworth & DR Dewey), pubescent wheatgrass (*Agropyron trichophorum* (Link) Richter), tall wheatgrass (*Thinopyrum poticum* (Podp.) Z.-W. Liu & R.-C. Wang) and alfalfa (*Medicago sativa* L.).

### 2.2. Field data

The 8.1 ha CRP pasture was divided into nine 0.9 ha plots and six sampling points were randomly selected within each plot. We sampled at three phenological stages: boot, peak growth, and dormancy. The boot stage was defined at the point at which the inflorescence of grass was enclosed by the sheath of the uppermost part of the plant; peak growth was defined as when the grass was 50% flowering and alfalfa had reached 7–8% bloom; and dormancy was when the study area had received at least one week of temperature below 0 °C. When the plants reached the appropriate growth stage (boot, peak growth, and dormancy), a 1 m<sup>2</sup> quadrat at each of the randomly selected points was scanned by the active ground based remote sensing unit Crop Circle (model ACS 470, Holland Scientific) [24]. Then the biomass was hand clipped to within 2.5 cm of the soil to mimic the effects from grazing. The measurements were conducted in mid-May to early June, late June to early July, and mid- to late October corresponding to the phenological growth stages of boot, peak growth, and dormancy, respectively. Quadrats were scanned and clipped only once. We took 54 samples at the boot stage, 27 at peak growth, and 27 at dormancy because one-half of the field plots were harvested at the peak growth stage. This process was repeated in each of the two years in 2011 and 2012, resulting in a total of 216 samples. The biomass samples were dried at 40.6 °C for 72 h. Total dry biomass production per 1 m<sup>2</sup> quadrat was then weighed, recorded, and used to determine dry biomass production in kg ha<sup>-1</sup>.

### 2.3. Spectral data

The Crop Circle sensor is an active multichannel sensor that records reflected energy in the red (0.66–0.68 μm), red edge (0.72–0.74 μm), and near infrared (NIR) (0.76–0.81 μm) portions of the spectrum [24]. NDVI from the Crop Circle sensor was calculated from energy reflectance in the red and NIR bands using the formula:  $NDVI = (NIR - Red)/(NIR + Red)$  [12]. The sensor was operated from 1 m above the vegetation, and has an instantaneous field-of-view that is approximately 30° by 14° [24]. Thus, we captured an area of 0.125 m<sup>2</sup> (0.5 m by 0.25 m) simultaneously. We made two passes to completely scan the 1 m<sup>2</sup> quadrat. The Crop Circle sensor generates its own source of illumination and is not affected by ambient lighting conditions [24]; therefore, radiometric normalization was not necessary.

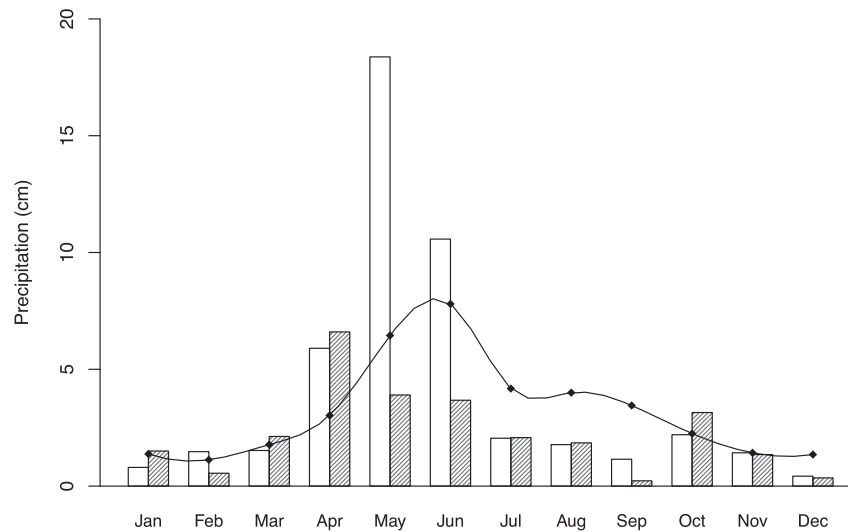


**Fig. 1 – Monthly precipitation for 2011 (white bars), 2012 (shaded bars) and the smoothed 103-year historical average (black line) [22].**

Landsat 5 and 7 images were acquired from the United States Geological Survey (USGS) [25] and were within 14 days of the field collection date for the boot and peak growth stages, and within 30 days for dormancy (Table 1). When directly comparing images from different dates, exogenous factors, such as differences in atmospheric conditions or solar zenith angles affect the amount of reflected radiation [26]. To account for this variation, all images were radiometrically normalized to the 4 June 2011 image using pseudo-invariant features [26].

The sensor aboard the Landsat 5 satellite was the Thematic Mapper (TM), while Landsat 7 carries the Enhanced Thematic Mapper Plus (ETM+). Both sensors record reflected energy in seven spectral bands. We refer hereafter to TM and ETM+ spectral bands by band number: band 1 = blue (0.45–0.52  $\mu\text{m}$ ), band 2 = green (0.52–0.60  $\mu\text{m}$ ), band 3 = red (0.63–0.69  $\mu\text{m}$ ), band 4 = near infrared (0.75–0.90  $\mu\text{m}$ ), band 5 = short-wave infrared (1.55–1.75  $\mu\text{m}$ ), band 6 = thermal (10.4–12.5  $\mu\text{m}$ ), and band 7 = short-wave infrared (2.09–2.35  $\mu\text{m}$ ) [27]. Reflectance values for bands 1–7 were extracted from the pixels that

contained a quadrat. NDVI was calculated in the same manner as with the Crop Circle sensor. Dry biomass measurements from the quadrats were used to represent the biomass produced in each pixel [13]. Since TM and ETM+ pixels are 900  $\text{m}^2$  (30 m  $\times$  30 m) in area, the 1  $\text{m}^2$  quadrats represent the biomass produced in a much larger area and we make the necessary assumption that the quadrats are unbiased and representative of the larger area [13,27].

#### 2.4. Analysis

Biomass was estimated with multiple linear regression models in which the explanatory variables were either NDVI, or spectral reflectance values and their two-way interactions. The reflectance values from each spectral band were the explanatory variables in the regression equations, and they are often highly correlated, either high pair-wise correlations or high multiple-correlation between one variable and several others. These relationships are indicative of potentially significant interactions [28]; therefore, we used all possible two-way interactions in the full model. We generated two NDVI and two bandwise regression models from Crop Circle and Landsat data, resulting in a total of four full models (Table 2). Bandwise regression (forward and backward) was used on the full models to remove non-significant bands, which produced the set of reduced models (Table 3). We used indicator variables to denote the peak growth and dormancy phenological stages ( $I_p$  and  $I_d$  respectively) – the boot stage does not need an indicator as it was the baseline.

The data from each year were pooled and one-half of the observations from each growth stage was used to build the models, while the remaining observations were used to test the models' ability to estimate actual biomass. Five observations were removed from the subset used to build the models because the quadrats were located in Landsat 7 ETM+ data gaps. These data gaps are caused by the failure of the scan line corrector, which compensates for forward motion while the

**Table 1 – Differences in days between image acquisition and biomass clipping.<sup>a</sup>**

Year & phenological stage	Sensor	Image date	Clipping date	Difference
2011 – Boot stage	TM	4 Jun 2011	3 Jun 2011	1
2011 – Peak growth	ETM+	28 Jun 2011	1 Jul 2011	3
2011 – Dormancy	TM	26 Sep 2011	27 Oct 2011	1
2012 – Boot stage	ETM+	13 May 2012	8 May 2012	5
2012 – Peak growth	ETM+	14 Jun 2012	28 Jun 2012	14
2012 – Dormancy	ETM+	18 Sep 2012	18 Oct 2012	30

<sup>a</sup> TM = Thematic Mapper (Landsat 5 sensor), ETM+ = Enhanced Thematic Mapper Plus (Landsat 7 sensor).

**Table 2 – Full biomass models.<sup>a</sup>**

Bandwise regression models	
Landsat	$\beta_0 + B1 + B2 + B3 + B4 + B5 + B6 + B7 + I_p + I_d + (B1 \cdot I_p) + (B2 \cdot I_p) + (B3 \cdot I_p) + (B4 \cdot I_p) + (B5 \cdot I_p) + (B6 \cdot I_p) + (B7 \cdot I_p) + (B1 \cdot I_d) + (B2 \cdot I_d) + (B3 \cdot I_d) + (B4 \cdot I_d) + (B5 \cdot I_d) + (B6 \cdot I_d) + (B7 \cdot I_d) + (B1 \cdot B2) + (B1 \cdot B3) + (B1 \cdot B4) + (B1 \cdot B5) + (B1 \cdot B6) + (B1 \cdot B7) + (B2 \cdot B3) + (B2 \cdot B4) + (B2 \cdot B5) + (B2 \cdot B6) + (B2 \cdot B7) + (B3 \cdot B4) + (B3 \cdot B5) + (B3 \cdot B6) + (B3 \cdot B7) + (B4 \cdot B5) + (B4 \cdot B6) + (B4 \cdot B7) + (B5 \cdot B6) + (B5 \cdot B7) + (B6 \cdot B7)$
Crop circle	$\beta_0 + R + NIR + RE + I_p + I_d + (R \cdot I_p) + (R \cdot I_d) + (NIR \cdot I_p) + (NIR \cdot I_d) + (RE \cdot I_p) + (RE \cdot I_d) + (R \cdot NIR) + (R \cdot RE) + (NIR \cdot RE)$
NDVI-based models	
Landsat	$\beta_0 + NDVI + I_p + I_d + (NDVI \cdot I_p) + (NDVI \cdot I_d)$
Crop circle	$\beta_0 + NDVI + I_p + I_d + (NDVI \cdot I_p) + (NDVI \cdot I_d)$

<sup>a</sup> The intercept is  $\beta_0$ , the undetermined coefficients ( $\beta_i$ ) have been eliminated from all other variables for simplicity.  $I_p$  and  $I_d$  are indicator variables for peak growth and dormancy (there is no indicator for the boot stage as this was the baseline). The boot stage was the point at which the inflorescence was enclosed by the sheath of the uppermost part of the plant; peak growth was when the alfalfa had reached 7–8% bloom; and dormancy was when the study area had received at least one week of temperature below 0 °C. NDVI = normalized difference vegetation index. R, NIR and RE refer to the red, near-infrared, and red-edge bands of the crop circle sensor. B1–B7 indicate Landsat bands 1–7. Two-way interactions are in parentheses.

sensor scans back and forth; the result is diagonal bands of no data on ETM+ images [27]. For the same reason, 12 observations were removed from the validation subset, which reduced the number of observations from 108 to 96. Coefficients of determination ( $R^2$ ) were used to estimate the amount of explained variance in each model and provide a measure of goodness-of-fit [13,21].

Actual biomass values were regressed against the estimated biomass values from each regression model to assess model accuracy. We also used two-sample t-tests to determine if a statistically significant difference ( $\alpha = 0.05$ ) in means existed between actual and estimated biomass values. Results from these t-tests suggested whether or not the models were predicting within the bounds of uncertainty and supplemented the model accuracy assessments. Averages for actual and estimated biomass, as well as their differences, standard errors and confidence intervals were calculated for each model. Finally, actual biomass values were regressed against estimated biomass by growth stage.

### 3. Results and discussion

The reduced models fit the calibration data reasonably well with moderate to high  $R^2$  values (Table 3; Fig. 2). The bandwise regression models from each sensor explained more variance

than the NDVI-based sensors; 0.84 versus 0.65 for Landsat, and 0.73 versus 0.69 for the Crop Circle sensor. This is likely due to the larger number of explanatory variables and, for Landsat, the inclusion of the short-wave infrared bands. The reduced Landsat bandwise regression model had a total 28 explanatory variables. In contrast, the reduced Crop Circle bandwise regression model used nine explanatory variables, whereas the reduced NDVI-based models, from either sensor, used only five explanatory variables. Bandwise regression with the Landsat data was the only model that incorporated data from the short-wave infrared bands (bands 5 and 7), which are associated with the water content within a plant such that higher reflectance values indicate drier vegetation.

The mean value for actual biomass across all growth stages for 2011 and 2012 was  $2476 \pm 169 \text{ kg ha}^{-1}$  and each of the four models performed well at estimating this value (Table 4). All estimates were within  $276 \text{ kg ha}^{-1}$  of the actual value. The Landsat-derived NDVI model gave the most accurate estimate with a difference of only  $22 \pm 96 \text{ kg ha}^{-1}$ . The next best estimates were from the Landsat bandwise regression model ( $83 \pm 90 \text{ kg ha}^{-1}$ ), Crop Circle bandwise regression ( $155 \pm 90 \text{ kg ha}^{-1}$ ), and the Crop Circle NDVI model ( $182 \pm 94 \text{ kg ha}^{-1}$ ). Nonetheless, estimated biomass from the ‘worst’ performing model (Crop Circle – NDVI) was within 8% of the actual measured value, while the ‘best’ model (Landsat – NDVI) produced estimates within 1%. Both Landsat-derived

**Table 3 – Reduced (final) biomass models.<sup>a</sup>**

Bandwise regression models		Adj. $R^2$
Landsat	$-129,400.0 + 1242.0 * B1 + 418.1 * B2 - 132.5 * B3 + 999.5 * B4 - 300.0 * B5 + 736.0 * B6 - 129.7 * B7 + 3979.0 * I_p + 40,050.0 * I_d - 247.2 * (B1 \cdot I_p) + 379 * (B3 \cdot I_p) + 190.2 * (B4 \cdot I_p) - 490.9 * (B5 \cdot I_p) + (B6 \cdot I_p) + 786.7 * (B7 \cdot I_p) + 682.7 * (B2 \cdot I_d) + 718.6 * (B3 \cdot I_d) + 515.4 * (B5 \cdot I_d) + 251.5 * (B6 \cdot I_d) + 1064 * (B7 \cdot I_d) - 7.3 * (B1 \cdot B3) - 18.5 * (B1 \cdot B5) - 5.0 * (B1 \cdot B6) + 42.2 * (B1 \cdot B7) - 12.5 * (B2 \cdot B4) + 10.9 * (B2 \cdot B5) + 38.7 * (B3 \cdot B5) - 89.4 * (B3 \cdot B7) - 4.4 * (B4 \cdot B6)$	0.84
Crop circle	$-967.3 - 3795.2 * R + 4916.4 * NIR + 13,215.6 * RE + 1471.6 * I_p - 3619.1 * I_d + 127,054.3 * (R \cdot I_d) - 58,598.6 * (NIR \cdot I_d) - 49,525.0 * (RE \cdot I_d) - 27,093.9 * (R \cdot RE)$	0.73
NDVI-based models		
Landsat	$628.2 + 1514.5 * NDVI + 799.3 * I_p - 3804.6 * I_d + 3458.1 * (NDVI \cdot I_p) + 49,391.0 * (NDVI \cdot I_d)$	0.65
Crop circle	$-444.8 + 6918.6 * NDVI - 125.8 * I_p + 7462.4 * I_d + 6345.9 * (NDVI \cdot I_p) - 80,776.7 * (NDVI \cdot I_d)$	0.69

<sup>a</sup> As in Table 2, but the undetermined coefficients ( $\beta_i$ ) were added and non-significant variables dropped.

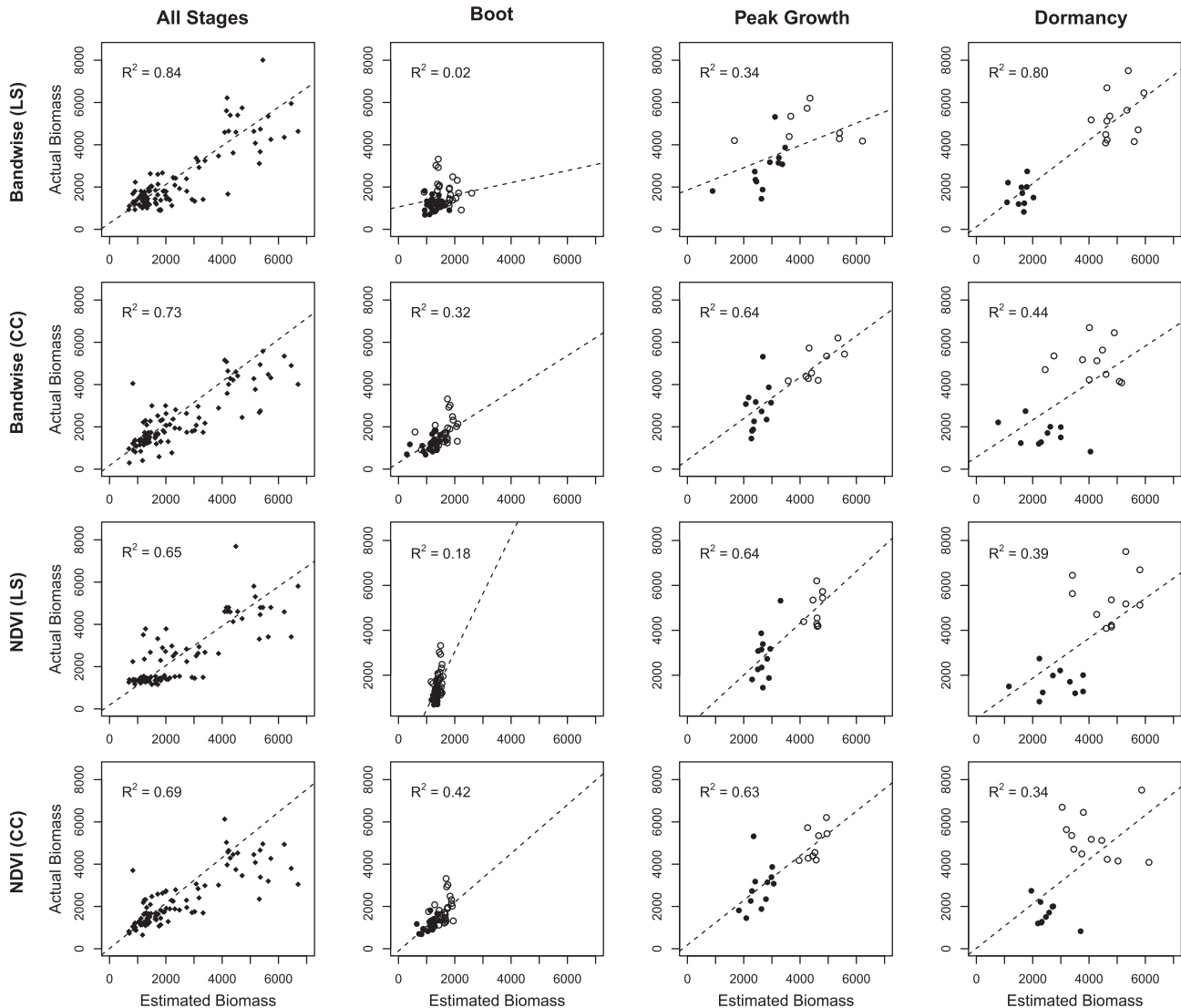


**Fig. 2** – Plots of actual biomass (y-axis) versus estimated biomass (x-axis) from the reduced models for all data (column 1) and by phenological stage (columns 2–4). Actual and estimated biomass are measured in  $\text{kg ha}^{-1}$ . LS = Landsat, CC = crop circle. NDVI = normalized difference vegetation index. The white circles indicate 2011 and the black circles are 2012. The boot stage was the point at which the inflorescence of grass was enclosed by the sheaf of the uppermost part of the plant; peak growth was when grass had reached 50% flowering and the alfalfa had reached 7–8% bloom; and dormancy was when the study area had received at least one week of temperature below  $0^\circ\text{C}$ . For all slopes,  $p < 0.01$ .

models produced better estimates than the corresponding models from the Crop Circle sensor, further supporting the value of additional bands. The spatial resolution of Landsat,  $900\text{ m}^2$ , was substantially larger than the  $1\text{ m}^2$  quadrats. Consequently, some samples had the same values for bands 1–7, as well as NDVI, because their quadrats were located in the same Landsat pixel. This reduced the amount of variability in the Landsat-based models. In contrast, the Crop Circle sensor had a spatial resolution less than  $1\text{ m}$ , which gave each quadrat a unique set of spectral measurements and increased variability in the Crop Circle-based models. Results from two-sample t-tests suggest that all models were predicting within the bounds of uncertainty as there were no statistically significant differences between estimated and actual biomass for any of the final models (Table 4).

Spectral values, and therefore NDVI, vary with phenological stage. As plants mature and progress through the different phenological stages of development, plant morphological features change [10,11], causing changes in spectral response. Consequently, we also examined the effect of phenology on biomass estimation models by regressing estimated and actual biomass against one another, grouped by phenological stage (Fig. 2). The models were not equally successful at estimating biomass when comparisons are made by phenological growth stage, suggesting that there are preferable times to estimate biomass depending on the available sensor. Overall, the best results came from bandwise regression with Landsat data at the dormancy stage ( $R^2 = 0.80$ ); however, it gave the poorest model estimates when applied to the boot stage ( $R^2 = 0.02$ ) because of the differences in

**Table 4 – Comparison of the reduced (final) models' ability to estimate biomass.<sup>a</sup>**

Reduced model	Actual biomass	Estimated biomass	Difference	95% CI	df	p-Value
Bandwise regression (Landsat)	2476 ± 169	2392 ± 157	83 ± 90	(–95, 261)	189	0.72
Bandwise regression (crop circle)	2476 ± 169	2321 ± 144	155 ± 90	(–23,333)	185	0.49
NDVI (Landsat)	2476 ± 169	2454 ± 149	22 ± 96	(–169, 212)	187	0.93
NDVI (crop circle)	2476 ± 169	2294 ± 131	182 ± 94	(–4, 368)	179	0.40

<sup>a</sup> All biomass values ( $\text{kg ha}^{-1}$ ) are mean ± SE with a sample size of 96. SE = standard error, CI = confidence interval and df = degrees of freedom. Difference refers to the absolute value of the difference between the actual and estimated values. The p-values are from two-sample t-tests – no model indicated a statistically significant difference between the actual and estimated biomass. NDVI = normalized difference vegetation index.

chlorophyll, plant water content, and vegetative canopy between boot and dormancy stages.

The peak growth stage showed moderately strong relationships ( $R^2 = 0.63$ – $0.64$ ) between actual and estimated biomass (Table 5; Fig. 2) in all models except bandwise regression with Landsat data ( $R^2 = 0.34$ ). The peak growth stage was characterized by photosynthetically active (green) plants. Green vegetation at peak growth contains high levels of chlorophyll and displays a distinctive inverse relationship between reflectance in the red and NIR portions of the spectrum [6]. NDVI was designed specifically to take advantage of this relationship [12]; consequently, NDVI-based models performed reasonably well at this stage.

Relationships between actual and estimated biomass were moderate in the dormancy stage with  $R^2$  values between 0.34 and 0.44 (Table 5; Fig. 2) for all models except bandwise regression with the Landsat data, which had a strong relationship ( $R^2 = 0.80$ ). The study area in the dormancy stage consisted of a mixture of dormant (senescent) vegetation and bare soil, which are more reflective in the visible and short-wave infrared regions [7]. As discussed earlier, Landsat incorporates two short-wave infrared bands that are associated with the water content of plants and, therefore, senescence. Models without the short-wave infrared bands had weaker relationships at this stage.

Relationships for the boot stage were typically poor to moderate with  $R^2$  values as low as 0.02 (Table 5; Fig. 2). The Crop Circle models showed the strongest relationships

between actual and estimated biomass ( $R^2 = 0.32$  and  $0.42$ ) at the boot stage. The Landsat models performed poorly at this stage ( $R^2 = 0.02$  and  $0.18$ ). The superior performance of the Crop Circle models at the boot stage is likely due to its finer spectral and spatial resolution. Spectrally, the Crop Circle sensor has a red edge band in the near infrared that corresponds to the point of maximum slope in vegetation reflectance spectra and it is sensitive to chlorophyll concentration [29]. The red edge ( $0.72$ – $0.74 \mu\text{m}$ ) is more narrowly defined than the broader Landsat near infrared band ( $0.75$ – $0.90 \mu\text{m}$ ). Furthermore, the much smaller sensor footprint of the Crop Circle sensor minimizes reflections from regions that might not yet be in the boot stage.

#### 4. Summary

Regression, both NDVI and bandwise regression models, was successfully constructed to estimate biomass in a CRP pasture. Regardless of the model or sensor, estimated values were within 8% of the measured biomass values; the best estimates were within 1%. Biomass estimation, at boot and peak growth stages, was most accurate with models using the red, red edge and NIR. Estimation at dormancy was most successful when models incorporated the short-wave infrared portion of the spectrum. Results demonstrated that models constructed from remotely sensed data can accurately estimate biomass over two consecutive growing seasons.

These techniques can be useful tools for land resource managers; however, the choice of an appropriate sensor remains. We only tested two sensors; there are many other satellite-based and hand-held options. The choice depends on several factors including the size of the land area, time of year, the sensor's spectral capabilities, and the cost of acquiring the data. We offer the following guidelines to help managers make an informed decision: (1) managers interested in assessing large areas should opt for satellite-based imagery such as Landsat, while small areas are likely better sensed with hand-held sensors; (2) the time of year for the assessment is important because NDVI only works well as long as plant chlorophyll is present (the early growing season through summer); autumn assessments are less reliable; (3) sensors with more bands (e.g., Landsat) tend to outperform those with fewer bands (e.g., many hand-held sensors), and fewer bands make it more likely that a manager will have to rely on NDVI rather than bandwise regression; and (4) satellite-based imagery is typically freely available, whereas hand-held sensors

**Table 5 – Reduced (final) model performance (adjusted  $R^2$ ) of estimating biomass by growth stage.<sup>a</sup>**

Reduced model	$R^2$		
	Boot stage	Peak growth	Dormancy
Bandwise regression (Landsat)	0.02	0.34	0.80
Bandwise regression (crop circle)	0.32	0.64	0.44
NDVI (Landsat)	0.18	0.64	0.39
NDVI (crop circle)	0.42	0.63	0.34

<sup>a</sup> NDVI = normalized difference vegetation index. The boot stage was the point at which the inflorescence was enclosed by the sheath of the uppermost part of the plant; peak growth was when the alfalfa had reached 7–8% bloom; and dormancy was when the study area had received at least one week of temperature below  $0^\circ\text{C}$ .

must be purchased. We note that more research is needed to determine the spatial and temporal robustness of our findings.

## Acknowledgments

The authors thankfully acknowledge the Montana State University Central Agricultural Research Station staff, specifically Dave Wichman, Superintendent of the Research Station, and Johnna Hesel, field technician, for their help with field data collection and the use of assets at the research station. We also thank the Montana State University Animal and Range Sciences Department for the use of facilities and financial support. Funding support for this project came from the North Central Regional Sun Grant Center at South Dakota State University through a grant provided by the USDOE Office of Biomass Programs under Award no. DE-FC36-05G085041 and the Montana State Agricultural Experiment Station.

## REFERENCES

- [1] Hess JR, Foust TD, Graham R, Sokhansanj S. Roadmap for agricultural biomass feedstock supply in the United States [Report No DOE/NE-ID-11129 Rev 1]. Washington DC: United States Department of Energy, Energy Efficiency and Renewable Energy; November 2003. p. 100.
- [2] Perlack RD, Stokes BJ. US billion-ton update: biomass supply for a bioenergy and bioproducts industry [ORNL/TM-2011/224]. Oak Ridge (TN): Oak Ridge National Laboratory; August 2011. p. 227. Prepared of the USDOE under contract DE-AC05-00OR22725.
- [3] Farm Service Agency. Conservation reserve program [Internet]. Washington DC: United States Department of Agriculture; 2013. Available from: <http://www.fsa.usda.gov/FSA/webapp?area=home&subject=copr&topic=crp> [accessed 20.09.13].
- [4] Summary of active and expiring CRP cropland acres by state – CRP – monthly contracts report. Montana FSA State Office, P.O. Box 670, Bozeman, MT 59771. (406) 587 6881.
- [5] Weiser RL, Asrar G, Miller GP, Kanemasu ET. Assessing grassland biophysical characteristics from spectral measurements. *Rem Sens Environ* 1986;20(2):141–52.
- [6] Knipling EB. Physical and physiological basis for the reflectance of visible and near-infrared radiation from vegetation. *Rem Sens Environ* 1970;1:155–9.
- [7] Todd SW, Hoffer RM, Michunas DG. Biomass estimation on grazed and ungrazed rangeland using spectral indices. *Int J Rem Sens* 1998;19:427–38.
- [8] Morrison IM. Changes in the lignin and hemicellulose concentrations of ten varieties of temperate grasses with increasing maturity. *Grass Forage Sci* 1980;35:287–93.
- [9] Nordkvist E, Aman P. Changes during growth in anatomical and chemical composition and in vitro degradability of Lucerne. *J Sci Food Agric* 1986;37:1–7.
- [10] Fahey GC, Collins M, Mertens DR, Moser LE. Forage quality, evaluation, and utilization. Madison, WI: American Society of Agronomy, Inc.; 1994.
- [11] Taiz L, Zeiger E. Plant physiology. 5th ed. Sunderland, MA: Sinauer Associates, Inc.; 2010.
- [12] Rouse JW, Haas RH, Deering DW, Schell JA. Monitoring the vernal advancement and retrogradation (green wave effect) of natural vegetation [Report no. NASA/GSFC progress report RSC 19782]. Greenbelt, MD: National Aeronautics and Space Administration; 1973. p. 87.
- [13] Maynard CL, Lawrence RL, Nielsen GA, Decker G. Modeling vegetation amount using bandwise regression and ecological site descriptions as an alternative to vegetation indices. *Glsci Rem Sens* 2006;43:1–14.
- [14] Teal RK, Tubana B, Girma K, Freeman KW, Arnall DB, Walsh O, et al. In season prediction of corn grain yield potential using normalized difference vegetation index. *Agron J* 2006;98:1488–94.
- [15] Raun WR, Solie JB, Johnson GV, Stone ML, Lukina EV, Thomason WE, et al. In season prediction of potential grain yield in winter wheat using canopy reflectance. *Agron J* 2001;93:131–8.
- [16] Stamatiadis S, Taskos D, Tsadilla E, Christofides C, Tsadilas C, Schepers JS. Comparison of passive and active canopy sensors for the estimation of vine biomass production. *Precis Agric* 2010;11:306–15.
- [17] Paruelo JM, Epstein HE, Lauenroth WK, Burke IC. ANPP estimates from NDVI for the central grassland region of the United States. *Ecology* 1997;78:953–8.
- [18] Flynn SE, Dougherty CT, Wendroth O. Assessment of pasture biomass with the normalized difference vegetation index from active ground based sensors. *Agron J* 2008;100:114–21.
- [19] Todd SW, Hoffer RM. Responses of spectral indices to variations in vegetation cover and soil background. *Photogramm Eng Rem Sens* 1998;64(9):915–21.
- [20] Flynn SE. Using NDVI as a pasture management tool [Thesis]. Lexington, KY: University of Kentucky; 2006.
- [21] Lawrence RL, Ripple WJ. Comparisons among vegetation indices and bandwise regression in a highly disturbed, heterogeneous landscape: Mount St. Helens, Washington. *Rem Sens Environ* 1998;64:91–102.
- [22] Montana State University. Weather data [Internet]. Bozeman, MT: Montana State University Central Agricultural Research Center; 2013. Available at: <http://ag.montana.edu/carc/Weather.html> [accessed 20.09.13].
- [23] Chen C, Neill K, Wichman D, Westcott M. Hard red spring wheat response to row spacing, seeding rate, and nitrogen. *Agron J* 2008;100:1296–302.
- [24] Holland Scientific. Crop circle ACS-470 multi-spectral crop canopy sensor [Internet]. Lincoln, NE: Holland Scientific, Inc.; 2013. Available at: <http://hollandscientific.com/crop-circle-acs-470-multi-spectral-crop-canopy-sensor/> [accessed 20.09.13].
- [25] United States Geological Survey. USGS global visualization viewer [Internet]. Sioux Falls, SD: US Department of the Interior, US Geological Survey, Earth Resources Observation and Science Center; 2013. Available at: <http://glovis.usgs.gov/> [accessed 12.02.13].
- [26] Collins JG, Woodcock CE. An assessment of several linear change detection techniques for mapping forest mortality using multitemporal Landsat TM data. *Rem Sens Environ* 1996;56:66–77.
- [27] United States Geological Survey. Landsat enhanced thematic mapper plus (ETM+) [Internet]. Sioux Falls, SD: US Department of the Interior, US Geological Survey, Earth Resources Observation and Science Center; 2013. Available at: <https://lta.cr.usgs.gov/LETMP> [accessed 12.09.13].
- [28] Kushla JD, Ripple WJ. Assessing wildfire effects with Landsat thematic mapper data. *Int J Rem Sens* 1998;19(3):2493–507.
- [29] Fillella I, Penuelas J. The red edge and shape indicators of plant chlorophyll content, biomass and hydric status. *Int J Rem Sens* 1994;15(7):1459–70.